Mandelpinski Structures in the Parameter Planes of Rational Maps *

Robert L. Devaney[†]
Department of Mathematics
Boston University
111 Cummington Mall
Boston, MA 02215 USA

October 12, 2015

*2000 MSC number: Primary 37F10; Secondary 37F45
[†]Robert L. Devaney was partially supported by Simons Foundation Grant #208780

Abstract

In this paper we give three examples of "Mandelpinski structures" that arise in the parameter planes for maps of the form $z^n + \lambda/z^d$. These structures include Mandelpinski necklaces, Mandelpinski spokes, and a Mandelpinski maze. We use the term "Mandelpinski" here since each of these objects consists of a variety of curves in the parameter plane that alternately pass through a large number of Mandelbrot sets and Sierpinski holes.

In this paper we give a survey of three different types of "Mandelpinski structures" that arise in the parameter planes for maps of the form

$$F_\lambda(z) = z^n + \frac{\lambda}{z^d}$$

where $n, d \geq 2$. Roughly speaking, a Mandelpinski structure is a collection of curves along which alternate a large number of Mandelbrot sets and Sierpinski holes. A Sierpinski hole is a disk in the parameter plane in which each parameter corresponds to a map whose Julia set is a Sierpinski curve, i.e., the Julia set is homeomorphic to the well known Sierpinski carpet fractal.

The types of curves that the Mandelbrot sets and Sierpinski holes alternate along can be very different. The first case we shall consider are Mandelpinski necklaces. When $n = d > 2$, these consist of infinitely many disjoint simple closed curves surrounding the origin in the λ-plane that contain more and more Mandelbrot sets and Sierpinski holes as the necklaces get smaller. See Section 2.

The second case involves Mandelpinski spokes (Section 4). In this case we assume $n \geq 2$ is even and $d \geq 3$ is odd. We first describe an infinite collection of Mandelbrot sets $\mathcal{M}^k$. Then we show that there are infinitely many disjoint arcs extending away from each $\mathcal{M}^k$ in different directions, and each arc now passes alternately through infinitely many Mandelbrot sets and Sierpinski holes. Attaching these sets to the arcs yields the Mandelpinski spokes.

In the third case we again assume that $n \geq 2$ is even and $d \geq 3$ is odd and show that there is a Mandelpinski maze in the parameter plane for this family. This result is described in Section 5. This maze consists of a sequence of planar graphs of increasing complexity. At each stage, each vertex on the graph corresponds to a different Mandelbrot set and the middle of each edge corresponds to a Sierpinski hole. To construct the next phase of the maze, at each vertex we "duplicate" the current graph centered at the given Mandelbrot set and then attach this additional graph to this Mandelbrot set to further extend the maze. See Figure 1 for a picture of each of these structures.

We will not provide complete proofs of all of these results in this paper. Rather, we will simply show how certain structures arise in the dynamical plane and then illustrate how ideas from complex analysis allow us to reproduce similar versions in the parameter plane. This follows what Adrien Douady often said: "In complex dynamics, we sow the seeds in the dynamical plane and reap the harvest in the parameter plane."

1 Preliminaries

In this paper we consider the family of rational maps given by

$$F_\lambda(z) = z^n + \frac{\lambda}{z^d}$$

where $n, d \geq 2$. When $|z|$ is large, we have that $|F_\lambda(z)| > |z|$, so the point at ∞ is an attracting fixed point in the Riemann sphere. We denote the immediate basin of attraction of ∞ by B_λ. There is also a pole at the origin for each of these maps, and so there is a neighborhood of the origin that is mapped into B_λ. If the preimage of B_λ surrounding the origin is disjoint from B_λ, we call this region the trap door and denote it by T_λ.

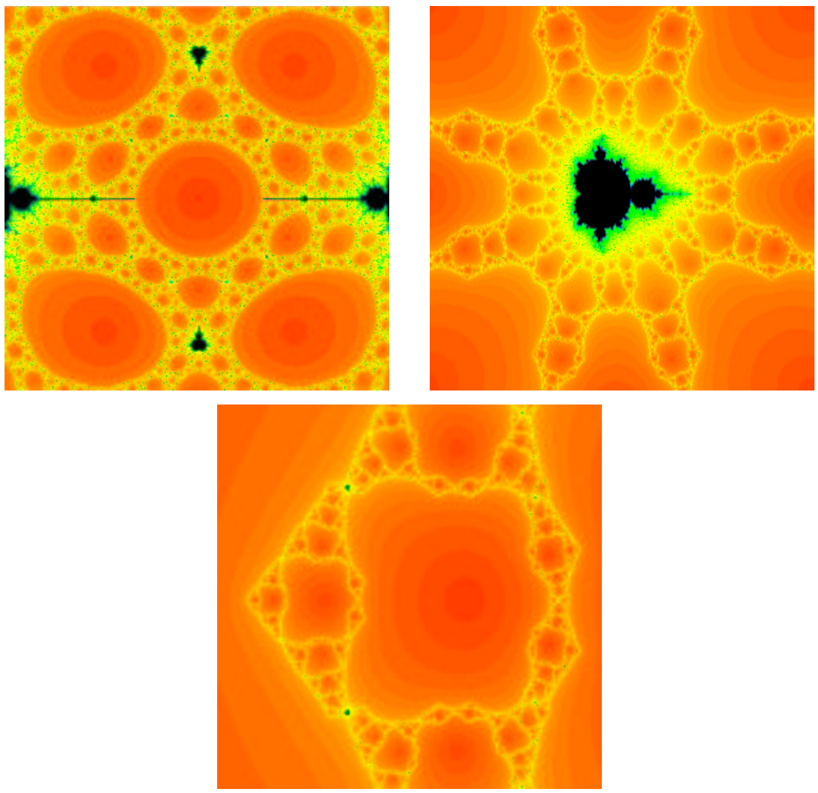

Figure 1: In this figure we display (a) some Mandelpinski necklaces for the family $z^3 + \lambda/z^3$; (b) the Mandelpinski spokes for the family $z^2 + \lambda/z^3$; and (c) a portion of the Mandelpinski maze for the family $z^2 + \lambda/z^3$. To see the Mandelbrot sets in each case usually requires many zooms into these images.

The Julia set of F_λ, $J(F_\lambda)$, has several equivalent definitions. $J(F_\lambda)$ is the set of all points at which the family of iterates of F_λ fails to be a normal family in the sense of Montel. Equivalently, $J(F_\lambda)$ is the closure of the set of repelling periodic points of F_λ, and it is also the boundary of the set of all points whose orbits tend to ∞ under iteration of F_λ, not just those in the boundary of B_λ. See [18].

One checks easily that there are $n+d$ critical points that are given by

$$c^\lambda = \left(\frac{d\lambda}{n}\right)^{\frac{1}{n+d}}$$

with the corresponding critical values given by

$$v^\lambda = \frac{(d+n)\lambda^{\frac{n}{n+d}}}{d^{\frac{d}{n+d}} n^{\frac{n}{n+d}}}.$$

Note that, when $n = d$, there are only two critical values given by $\pm 2\sqrt{\lambda}$. There are also $n+d$ prepoles given by

$$p^\lambda = (-\lambda)^{\frac{1}{n+d}}.$$

Let ω be an $(n+d)^{\text{th}}$ root of unity. Then we have $F_\lambda(\omega z) = \omega^n F_\lambda(z)$, and so it follows that the dynamical plane is symmetric under the rotation $z \mapsto \omega z$. In particular, all of the critical orbits have "similar" fates. If one critical orbit tends to ∞, then all must do so. If one critical orbit tends to an attracting cycle of some period, then all other critical orbits also tend to an attracting cycle, though these other cycles may have different periods. Nonetheless, the points on these attracting cycles are all symmetrically located with respect to the rotation by ω. As a consequence, each of B_λ, T_λ, and $J(F_\lambda)$ are symmetric under rotation by ω. Similarly, one checks easily that the parameter plane is symmetric under the rotation $\lambda \mapsto \nu\lambda$ where ν is an $(n-1)^{\text{st}}$ root of unity. The parameter plane is also symmetric under complex conjugation $\lambda \mapsto \overline{\lambda}$.

There is an Escape Trichotomy [12] for this family of maps. The first scenario in this trichotomy occurs when one and hence, by symmetry, all of the critical values lie in B_λ. In this case it is known that $J(F_\lambda)$ is a Cantor set [12]. The corresponding set of λ-values in the parameter plane is denoted by $\mathcal{C}$ and called the Cantor set locus. The second scenario is that the critical values all lie in T_λ (which we assume is disjoint from B_λ). In this case the Julia set is a Cantor set of simple closed curves surrounding the origin. This can only happen when $n, d \geq 2$ but not both equal to 2 [17]. We call the region $\mathcal{E}^1$ in parameter plane where this occurs the "McMullen domain"; it is known that $\mathcal{E}^1$ is an open disk surrounding the origin [3]. The third scenario is that the orbit of a critical point enters T_λ at iteration 2 or higher. Then, by the above symmetry, all such critical orbits do the same. In this case, it is known that the Julia set is a Sierpinski curve [10], i.e., a set that is homeomorphic to the well known Sierpinski carpet fractal. The regions in the parameter plane for which this happens are the open disks that we call Sierpinski holes [8], [20]. If the critical orbits do not escape to ∞, then it is known [15] that the Julia set is a connected set. Thus we call the set of parameters for which the critical orbits either do not escape or else enter the trap door at iteration 2 or higher the connectedness locus. This is the region between $\mathcal{C}$ and $\mathcal{E}^1$. See Figure 2.

Proving that a Julia set is a Sierpinski curve is often quite easy. By a theorem of Whyburn [21], any planar set that is compact, connected, locally connected, nowhere dense, and has the property that any pair of complementary domains are bounded by simple closed curves that are pairwise disjoint is homeomorphic to the Sierpinski carpet. In complex dynamics, verifying the first four of these properties is, in many cases, trivial. See [4], [10] for more details.

In [2] and [9] it has been shown that there are $n-1$ principal Mandelbrot

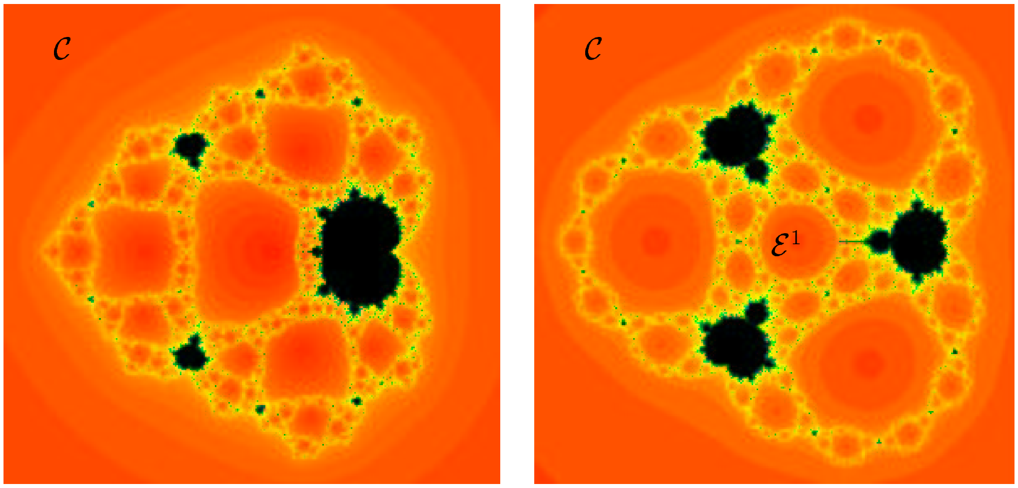

Figure 2: The parameter planes for the family $z^n + \lambda/z^d$ when $n = 2, d = 3$ and $n = 4, d = 3$. There is one principal Mandelbrot set in the first case and three symmetrically located such sets in the second. All of the red holes in these pictures (except the one surrounding the origin) are Sierpinski holes. $\mathcal{E}^1$ is too small to be seen in the first figure.

sets in the parameter plane for these maps. These are symmetrically located by the rotation $z \mapsto \nu z$ around the origin and extend from the Cantor set locus down to the McMullen domain.

For more details about the dynamical properties of these maps and the structure of the parameter plane, see [4].

2 Mandelpinski Necklaces

In this section we restrict attention to the family

$$F_\lambda(z) = z^n + \frac{\lambda}{z^n}$$

where $n \geq 3$. In this case the critical points of F_λ are given by $\lambda^{1/2n}$, the two critical values by $\pm 2\sqrt{\lambda}$, and the prepoles by $(-\lambda)^{1/2n}$. There is an additional symmetry in the dynamical planes for these maps. Let H_λ be an involution given by $\lambda^{1/n}/z$. Then $F_\lambda(H_\lambda(z)) = F_\lambda(z)$, so the dynamical plane is symmetric under each of these involutions.

Recall that, if $|\lambda|$ is small, the Julia set of F_λ is a Cantor set of simple closed curves surrounding the origin and the set of parameters for which this holds is the McMullen domain $\mathcal{E}^1$.

We define the center of a Sierpinski hole to be the unique parameter for which the orbits of the critical points all land on ∞, and the escape time is the number of iterations that it takes for the critical orbits to enter the trap door. The center of a Mandelbrot set is the unique superstable parameter that lies in the main cardioid.

The following result was proved in [13].

Theorem. *For each $k \geq 0$ there exists a simple closed curve C_k which surrounds the McMullen domain and the C_k converge to the boundary of this domain as $k \to \infty$. Each C_k passes alternately through exactly $(n-2)n^k + 1$ centers of Sierpinski holes with escape time $k+2$ and centers of baby Mandelbrot sets, i.e., very small copies of the usual Mandelbrot set.*

The center of a Sierpinski hole is the unique parameter for which the orbits of the critical points all land on ∞, and the escape time is the number of iterations that it takes for the critical orbits to enter the trap door. The center of a Mandelbrot set is the unique superstable parameter that lies in the main cardioid.

We call each C_k a *Mandelpinski necklace.* As a remark, this result also holds when $n = 2$ [1], but then the formula $(n-2)n^k + 1$ shows that each C_k passes through just one Sierpinski hole and one Mandelbrot set. Also, in a forthcoming paper by D. Cuzzocreo, it has been shown that each of the Sierpinski holes in the above result are known to be surrounded by infinitely many similar Mandelpinski sub-necklaces. And then this process continues

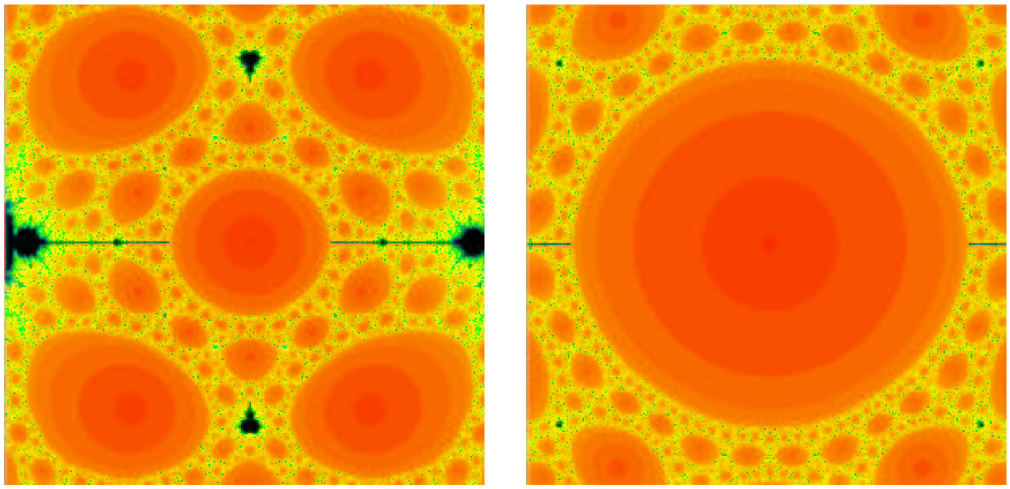

Figure 3: The rings around the McMullen domain in the family $z^3 + \lambda/z^3$. In each case, the McMullen domain is the central disk. The Sierpinski holes are visible in these rings, but most of the Mandelbrot sets are too small to be seen.

recursively with each sub-necklace having its own sub-necklaces. See Figure 3.

These Mandelpinski necklaces arise from the following structure in the dynamical plane. Let $\gamma_0 = \gamma_0^\lambda$ be the circle given by $|z| = |\lambda|^{1/2n}$ in the dynamical plane. So γ_0 contains all of the critical points and prepoles which are arranged along γ_0 in alternating fashion. We call γ_0 the *critical circle*. Note that each involution H_λ preserves the critical circle and interchanges the interior and exterior of this circle. One checks easily that F_λ maps the critical circle $2n$-to-one onto the *critical value segment* which is the straight line segment connecting the two critical values and hence passing through 0.

The first necklace C_0 then arises when the critical values lie on γ_0. This occurs when $|v^\lambda| = 2|\sqrt{\lambda}| = |\lambda|^{1/2n} = |c^\lambda|$. The necklace C_0 is the circle in the parameter plane given by $|\lambda| = (1/4)^{n/n-1}$. We call this the *dividing circle*. As λ rotates one full turn around the dividing circle, each crtical value rotates one-half a turn along γ_0, while each of the prepoles and critical points rotates only $(1/2n)^{\text{th}}$ of a turn. This shows that there are exactly $n-1$ centers of Sierpinski and baby Mandelbrot sets on C_0.

For the remaining necklaces, we assume that λ lies strictly inside the dividing circle in the parameter plane, so $|v^\lambda| < |c^\lambda|$. Therefore the critical circle is mapped strictly inside itself. As a consequence, the exterior of the critical circle is mapped as an n-to-one covering of the exterior of the critical value segment. Indeed, any circle outside γ_0 is mapped n-to-one onto an ellipse whose foci are $\pm v^\lambda$. Thus there is a preimage γ_1 of the critical circle that lies outside of γ_0. Then γ_1 contains $2n^2$ pre-critical points and the same number of pre-prepoles. Then the exterior of γ_1 is mapped as an n-to-one covering of the exterior of γ_0 and so there is another simple closed curve γ_2 that is mapped n-to-one onto γ_1. Thus γ_2 contains $2n^3$ points that are mapped to the critical points by F_λ^2 and the same number of points that are mapped to prepoles by F_λ^2. And this continues to produce a sequence of simple closed curves γ_k converging outward from γ_0 as $k \to \infty$, and each γ_k contains similar sets of $2n^{k+1}$ pre-critical points and prepoles.

By the H_λ symmetry, the interior of γ_0 is also mapped n-to-one onto the complement of the critical value segment. So we now have infinitely many other simple closed curves $\gamma_{-j}, j = 1, \ldots \infty$ lying inside γ_0. The curve γ_{-j} is mapped n-to-one onto γ_{j-1} and so these curves contain a similar number of points that are mapped to the critical points and prepoles by F_λ^j.

We then "transfer" this picture to the parameter plane as follows. As λ rotates once around the origin, a certain number of the preimages of the critical points and prepoles in C_k (namely, $(n-2)n^k + 1$ such points) can be shown to remain in the upper half plane. Consider the subset of the parameter plane consisting of an open annulus bounded by a circle strictly inside the McMullen domain and the dividing circle. Then remove the positive real axis from this set to give a simply connected set $\mathcal{O}$ in the parameter plane. Then we have two maps defined on $\mathcal{O}$. One map is given by $\lambda \mapsto v^\lambda$. The second is given by selecting one of the prepoles (or pre-critical points) on γ_{-k}^λ which remain in the upper half plane as λ rotates, excluding the critical points that lie on the real axis when λ is positive. Call this point z_λ^k where z_λ^k is chosen to vary analytically with λ. So this map is $\lambda \mapsto z_\lambda^k$.

The map $V(\lambda) = v^\lambda$ is invertible on $\mathcal{O}$, so we can consider the map $\lambda \mapsto V^{-1}(z_\lambda^k)$ from $\mathcal{O}$ to $\mathcal{O}$. Then the Schwarz Lemma implies that this map has a unique fixed point in $\mathcal{O}$. This fixed point is then the parameter λ^* for which $v^{\lambda^*} = z_{\lambda^*}^k$, so for the parameter λ^*, either one of the critical points c_{λ^*} returns to a critical point at iteration $k+1$, or else the orbit of a critical point lands on 0 at iteration $k+2$. When n is even, this implies that, in the first case, the orbit of some critical point lands on itself and hence is periodic of period $k+1$, whereas, if n is odd, this critical point may return to itself or to its negative and thus, by the $z \mapsto -z$ symmetry, this period is either $k+1$ or $2(k+1)$. This produces the parameters lying at the centers of the Sierpinski holes and the centers of the main cardioids of the baby Mandelbrot sets. Finding such a center of a Mandelbrot set in the case we excluded above when λ is positive is straightforward, since both v^λ and c^λ lie on the real axis in this case. Full details of this proof may be found in [13].

Producing the entire Sierpinski holes in these cases involves quasi-conformal surgery, while producing the entire baby Mandelbrot sets involves polynomial-like maps [16]. We shall illustrate how this works when we create the Mandelpinski spokes in a later section.

3 Dynamics on Sierpinski Curve Julia Sets

The Mandelbrot sets centered on the Mandelpinski necklaces C_k where $k > 0$ are all “buried” in the sense that they do not extend out to the external boundary of the connectedness locus. It is known that any parameter drawn from the main cardioid of such a buried Mandelbrot set is also a Sierpinski curve [11]. Thus we have a total of $2(n-2)n^k + 2$ open disks along C_k for which the corresponding maps have Julia sets that are Sierpinski curves. Hence all of these Julia sets are homeomorphic to one another. So the natural question is: what about the dynamical behavior on these Julia sets? When is the dynamical behavior the same, i.e., when are the maps topologically conjugate to one another? And when is this behavior different?

Regarding these questions, first note that parameters drawn from the main cardioids of the Mandelbrot sets always have different dynamical behavior from those lying in Sierpinski holes, since, in the Mandelbrot set case, we have that the boundaries of the attracting basins are invariant under some iterate of F_λ, whereas only ∂B_λ is invariant under iterates of F_λ in the Sierpinski hole case.

It is known that any two parameters drawn from the same Sierpinski hole or main cardioid of a Mandelbrot set have conjugate behavior on their Julia sets [14], [20]. Regarding different Sierpinski holes (or main cardioids), it is also shown in [14] that only those that are symmetrically located in the parameter plane by a rotation by an $(n-1)^{\text{st}}$ root of unity or by complex conjugation contain parameters for which the dynamics are the same. The maps cannot be topologically conjugate on the Julia sets if they are drawn from different, non-symmetrically located disks.

So now the question is: What makes the dynamics different in the non-symmetrically located disks? This has been determined by Moreno Rocha in the Sierpinski hole case [19] where she produces a dynamical invariant for these maps. But this situation is still unresolved in the cardioid case.

As a remark, this conjugacy result holds for all Sierpinski holes (including those described in the following sections), not just those lying along the Mandelpinski necklaces. Indeed, it is known that there are exactly $(n-1)(2n)^{k-2}$ Sierpinski holes with escape time k for maps of the form $z^n+\lambda/z^n$ [8], [20]. As mentioned above, the escape time is the number of iterations for the critical orbits to enter the trap door. Then there are exactly $(2n)^{k-3}$ different conjugacy classes of these maps when n is even and $(2n)^{k-3}/2+2^{k-4}$ when n is odd [14]. This count of the number of Sierpinski holes arises from the fact that there is a unique center of each Sierpinski hole, i.e., a parameter for which $F_\lambda^k(c^\lambda)=0$. Hence this count reduces to finding the number of roots of a polynomial equation, all of whose roots are known to be simple.

4 Mandelpinski Spokes

For the remainder of this paper, in order to keep the notation simple, we will restrict attention to the family of maps

$$F_\lambda(z)=z^2+\frac{\lambda}{z^3}.$$

However, all of the following constructions go through with only minor changes for the more general family

$$F_\lambda(z)=z^n+\frac{\lambda}{z^d}$$

where $n\geq 2$ is even and $d\geq 3$ is odd.

4.1 The Initial Mandelpinski Arc

In this section, in preparation for the next two Mandelpinski structures, we shall construct a *Mandelpinski arc.* This will be an arc in the parameter plane that passes alternately along the spines of infinitely many baby Mandelbrot sets and through the centers of the same number of Sierpinski holes. By the spine of a Mandelbrot set we mean the analogue of the portion of the real axis lying in the usual Mandelbrot set associated with the quadratic family $z^2 + c$.

In this initial Mandelpinski arc, there will be infinitely many Mandelbrot sets $\mathcal{M}^k$ with $k \geq 2$ along this arc. Here k is the period of the attracting cycle for parameters drawn from the main cardioid of $\mathcal{M}^k$, i.e., the base period of $\mathcal{M}^k$. There will also be infinitely many Sierpinski holes $\mathcal{E}^k$ with $k \geq 1$ where k is the escape time in $\mathcal{E}^k$, i.e., the number of iterations it takes for the orbit of the critical points to enter T_λ. In this special case, the Mandelpinski arc will be the portion of the negative real axis in the parameter plane extending from the McMullen domain $\mathcal{E}^1$ down to the endpoint on the boundary of the connectedness locus in the left half plane. Then the Mandelbrot sets and Sierpinski holes will be arranged along this arc as follows:

$$\dots \mathcal{M}^4 < \mathcal{E}^3 < \mathcal{M}^3 < \mathcal{E}^2 < \mathcal{M}^2 < \mathcal{E}^1.$$

In each case there will be an interval of nonzero length between any adjacent Mandelbrot set and Sierpinski hole lying along this arc. The Mandelpinski spokes we construct later will emanate from each of the $\mathcal{M}^k$, and the proof of the existence of these spokes will be similar in spirit to the proof that we sketch here.

In Figure 4 we display the parameter plane for $z^2 + \lambda/z^3$. Along the negative real axis, there are infinitely many red disks that are visible: these are the Sierpinski holes in the Mandelpinski arc. Between any two Sierpinski holes, there is then a (very small) Mandelbrot set as well as many more Sierpinski holes, as shown in the magnification in this figure.

There are now five critical points for the map F_λ that are given by

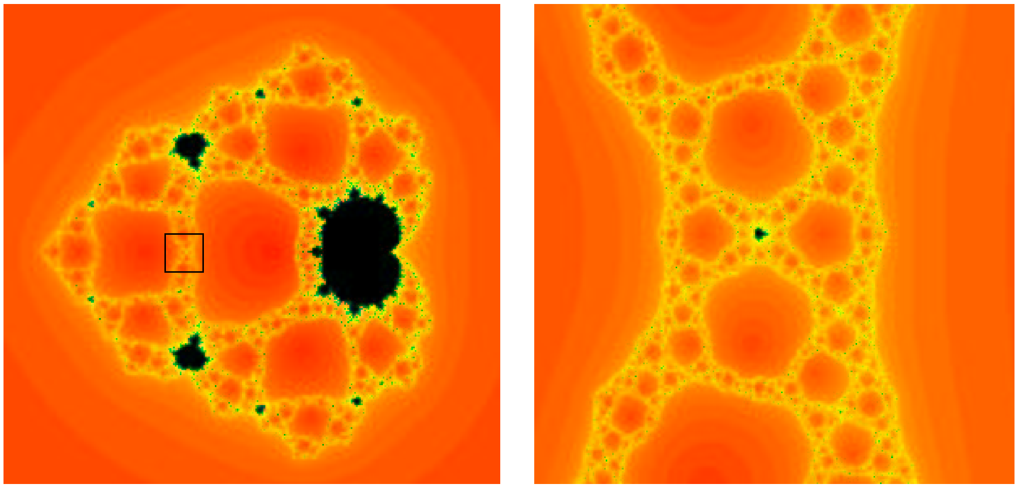

Figure 4: The parameter plane for $z^2 + \lambda/z^3$. The magnification shows a small Mandelbrot set between two of the large Sierpinski holes.

$(3\lambda/2)^{1/5}$. We denote the critical point that lies in $\mathbb{R}^-$ when $\lambda \in \mathbb{R}^-$ by $c_0 = c_0^\lambda$ (and then c_0^λ varies analytically with λ). We denote the other critical points by $c_j = c_j^\lambda$ for $-2 \leq j \leq 2$ where the c_j are now arranged in the clockwise order as j increases. As λ moves half way around the origin from $\mathbb{R}^-$, c_0 rotates exactly one-tenth of a turn in the corresponding direction. Thus, when $\operatorname{Arg}\lambda$ decreases from π to 0, c_2 lies in $\mathbb{R}^+$ and when $\operatorname{Arg}\lambda$ increases from π to 2π, c_{-2} now lies in $\mathbb{R}^+$. The critical values of F_λ are then given by $v^\lambda = \kappa\lambda^{2/5}$ where κ is the constant given by $5/(2^{2/5}3^{3/5})$. One computes easily that $\kappa \approx 1.96$. We denote by v_j^λ the critical value that is the image of c_j^λ.

There are also five prepoles for F_λ given by $(-\lambda)^{1/5}$. We denote the prepole that lies in $\mathbb{R}^+$ when $\lambda \in \mathbb{R}^-$ by $p_2 = p_2^\lambda$. The other prepoles are denoted by $p_j = p_j^\lambda$ where again $-2 \leq j \leq 2$ and the p_j are arranged in the clockwise order as j increases. Note that, when $\lambda \in \mathbb{R}^-$, the critical point c_0

lies between the two rays starting at the origin and passing through p_0 and p_{-1}. Unlike the previous case where $n = d$, the critical points and prepoles no longer lie on the same circle.

The straight ray extending from the origin to ∞ and passing through the critical point c_j^λ is a *critical point ray.* This ray is mapped two-to-one onto the portion of the straight ray from the origin to ∞ that starts at the critical value v_j^λ and extends to ∞. A similar straight line extending from 0 to ∞ and passing through a prepole p_j^λ is a *prepole ray*, and this ray is mapped one-to-one onto the entire straight line passing through both the origin and the point $(-\lambda)^{2/5}$.

To construct the objects lying along this Mandelpinski arc, we will restrict attention at first to the λ-values lying in the annular region $\mathcal{O}$ in parameter plane given by $10^{-10} \leq |\lambda| \leq 2$. Also, let $\mathcal{A}$ be the annulus in the dynamical plane given by $\kappa 10^{-4} \leq |z| \leq \kappa 2^{2/5}$ where $\kappa \approx 1.96$ is defined as above. Then easy estimates show that, for any $\lambda \in \mathcal{O}$, all points on the outer circular boundary of $\mathcal{A}$ lie in B_λ, while all points on the inner circular boundary of $\mathcal{A}$ lie in T_λ. Moreover, F_λ maps each of these boundaries strictly outside the boundary of $\mathcal{A}$. Also, if λ lies on the inner circular boundary of $\mathcal{O}$, then each critical value lies on the inner circular boundary of $\mathcal{A}$ and so λ lies in the McMullen domain. And, if λ lies on the outer circular boundary of $\mathcal{O}$, then each critical value lies on the outer circular boundary of $\mathcal{A}$ and so λ lies in the Cantor set locus in the parameter plane. For a detailed proof of this, see [6].

We now restrict attention to a "smaller" subset of $\mathcal{O}$. Let $\mathcal{O}'$ be the subset of $\mathcal{O}$ containing parameters λ for which $0 \leq \operatorname{Arg} \lambda \leq 2\pi$. Despite the overlap of this region along the real axis, we will think of $\mathcal{O}'$ as being a closed disk (not an annulus) in the parameter plane with $\operatorname{Arg} \lambda = 0$ and $\operatorname{Arg} \lambda = 2\pi$ considered as different portions of the boundary. We do this because, as

$\operatorname{Arg}\lambda$ increases from 0 to 2π, the critical point c_0 that we will be following rotates one-fifth of a turn in the dynamical plane. So this point will migrate to the position of a different critical point as $\operatorname{Arg}\lambda$ increases from 0 to 2π.

For any parameter in $\mathcal{O}'$, let L^λ be the closed "portion of the wedge" in the annulus $\mathcal{A}$ in the dynamical plane that is bounded by the two prepole rays through p_0 and p_{-1}. When $\lambda \in \mathbb{R}^-$, L^λ is thus bounded by the rays extending from 0 and passing through $\exp(2\pi i(2/5))$ and $\exp(2\pi i(3/5))$. So the critical point c_0 lies in the interior of L^λ. Next, let R^λ be the portion of the wedge in $\mathcal{A}$ that is bounded by the critical point rays passing through c_2 and c_{-2}. When $\lambda \in \mathbb{R}^-$, this wedge is bounded by the critical point rays extending from 0 and passing through $\exp(\pm 2\pi i/10)$. Note that R^λ is the symmetric image of L^λ under $z \mapsto -z$ for each $\lambda \in \mathcal{O}'$. See Figure 5.

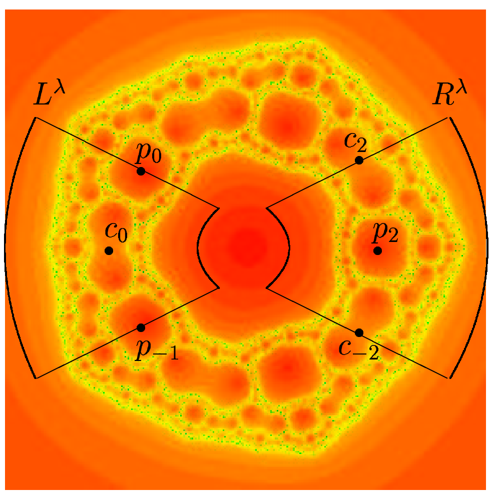

Figure 5: The wedges L^λ and R^λ for $\lambda = -0.09$.

Then it is easy to see that, for each $\lambda \in \mathcal{O}'$:

1. F_λ maps the interior of R^λ in one-to-one fashion onto a region that

contains the interior of $R^\lambda \cup L^\lambda$ together with a portion of T_λ that contains 0;

2. F_λ maps the interior of L^λ two-to-one over a region that contains the interior of R^λ;

3. As λ winds once around the boundary of $\mathcal{O}'$, the critical value $F_\lambda(c_0^\lambda) = v_0^\lambda$ winds once around the boundary of R^λ, (i.e., the winding index of the vector connecting this critical value to the prepole p_2^λ lying in the interior of R^λ is one).

Again, the details of this proof may be found in [6].

Before constructing this Mandelpinski arc, we recall the concept of a polynomial-like map. Let G_μ be a family of holomorphic maps that depends analytically on the parameter μ lying in some open disk $\mathcal{D}$. Suppose each $G_\mu : U_\mu \to V_\mu$ where both U_μ and V_μ are open disks that also depend analytically on μ. G_μ is then said to be polynomial like of degree 2 if, for each μ:

- G_μ maps U_μ two-to-one onto V_μ and so there is a unique critical point in U_μ;
- V_μ contains U_μ;
- As μ winds once around the boundary of $\mathcal{D}$, the critical value winds once around U_μ in the region $V_\mu - U_\mu$.

As shown in [16], for such a family of polynomial-like maps, there is a homeomorphic copy of the Mandelbrot set in the disk $\mathcal{D}$. Moreover, for μ-values in this Mandelbrot set, $G_\mu \,|\, U_\mu$ is conjugate to the corresponding quadratic map given by this homeomorphism.

To show the existence of the Mandelpinski arc in the parameter plane, we will first observe a "similar" collection of sets in the dynamical plane, and then use polynomial-like maps and the argument principle to produce the analogous Mandelbrot sets $\mathcal{M}^k$ and Sierpinski holes $\mathcal{E}^k$ in the parameter plane.

We shall first consider the escape time case. By construction, for each $\lambda \in \mathcal{O}'$, there is a unique prepole p_2^λ in the interior of R^λ. Since F_λ maps R^λ one-to-one over itself, there is a unique preimage of this prepole, z_3^λ, in R^λ, so $F_\lambda^2(z_3^\lambda) = 0$. Continuing, for each $\lambda \in \mathcal{O}'$, there is a unique point z_k^λ in R^λ for which we have $F_\lambda(z_k^\lambda) = z_{k-1}^\lambda$ and so $F_\lambda^{k-1}(z_k^\lambda) = 0$. Now the points z_k^λ vary analytically with λ and are strictly contained in the interior of R^λ. So we may consider the function $H^k(\lambda)$ defined on $\mathcal{O}'$ by $H^k(\lambda) = v_0^\lambda - z_k^\lambda$ where $v_0^\lambda = F_\lambda(c_0^\lambda)$. When λ rotates once around the boundary of $\mathcal{O}'$, v_0^λ rotates once around the boundary of R^λ while z_k^λ remains in the interior of R^λ. Hence $H^k(\lambda)$ has winding number one along the boundary of $\mathcal{O}'$ and so there must be a unique zero in $\mathcal{O}'$ for each H^k. This is then the parameter that lies at the center of the escape time region $\mathcal{E}^k$. It is well known [20] that $\mathcal{E}^k$ is then an open disk in the parameter plane. Note that, as λ decreases along $\mathbb{R}^-$, both v_0^λ and z_k^λ increase along $\mathbb{R}^+$. It then follows that the portion of $\mathcal{E}^{k+1}$ in $\mathbb{R}^-$ lies to the left of $\mathcal{E}^k$ in the parameter plane.

To prove the existence of the Mandelbrot sets $\mathcal{M}^k$, recall that the orbit of the point z_k^λ under F_λ remains in R^λ before entering T_λ and landing at 0 at iteration $k-1$ (here $z_2^\lambda = p_2^\lambda$). For each $k \geq 2$, let E_λ^k be the open set surrounding z_k^λ in R^λ that is mapped to T_λ by F_λ^{k-1}. Let D_λ^k be the set in R^λ consisting of points whose first $k-2$ iterations lie in R^λ but whose $(k-1)^{\text{st}}$ iterate lies in the interior of L^λ. Since F_λ is univalent on R^λ, each D_λ^k is an open disk. Furthermore, the boundary of D_λ^k meets a portion of the boundaries of both E_λ^{k-1} and E_λ^k (where $E_\lambda^1 = T_\lambda$). Since F_λ^{k-1} maps D_λ^k one-to-one over the interior of L^λ and then F_λ maps L^λ two-to-one over a region that contains R^λ, we have that F_λ^k maps D_λ^k two-to-one over a region that completely contains R^λ. Moreover, the critical value for F_λ^k is just v_0^λ, which, as mentioned above, winds once around the exterior of R^λ as λ winds once around the boundary of $\mathcal{O}'$. Hence F_λ^k is a polynomial-like map of degree two on D_λ^k and this proves the existence of a baby Mandelbrot set $\mathcal{M}^k$ lying in $\mathcal{O}'$ for each $k \geq 2$. When λ is real and negative, we have that the centers of the escape regions $\mathcal{E}^k$ lie along $\mathbb{R}^-$ and, since the real line is invariant under F_λ when $\lambda \in \mathbb{R}^-$, both c_0^λ and v_0^λ also lie on the real axis. Then, by the $\lambda \mapsto \overline{\lambda}$ symmetry in the parameter plane, the spines of these Mandelbrot sets also lie in $\mathbb{R}^-$.

Next, since the E_λ^k and D_λ^k are arranged along the postive real axis in the following fashion:

$$T_\lambda = E_\lambda^1 < D_\lambda^2 < E_\lambda^2 < D_\lambda^3 < E_\lambda^3 < \dots$$

and, as shown above, the $\mathcal{E}^k$ decrease along $\mathbb{R}^-$ as k increases, we therefore have that the $\mathcal{E}^k$ and $\mathcal{M}^k$ are arranged along the negative real axis in the parameter plane in the opposite manner:

$$\dots \mathcal{E}^3 < \mathcal{M}^3 < \mathcal{E}^2 < \mathcal{M}^2 < \mathcal{E}^1.$$

See Figure 6.

4.2 Construction of the Mandelpinski Spokes

In this section, we shall concentrate on a specific Mandelbrot set $\mathcal{M}^k$ and describe the infinite collection of Mandelpinski spokes emanating from this set. A *Mandelpinski spoke* is an arc in the parameter plane along which lie infinitely (or finitely) many Mandelbrot sets and Sierpinski holes in alternating fashion. With an eye toward how we shall proceed with this construction, note that, at this stage, we have already produced a single infinite Mandelpinski spoke extending to the left of $\mathcal{M}^k$ which contains the sets $\mathcal{M}^j$ with

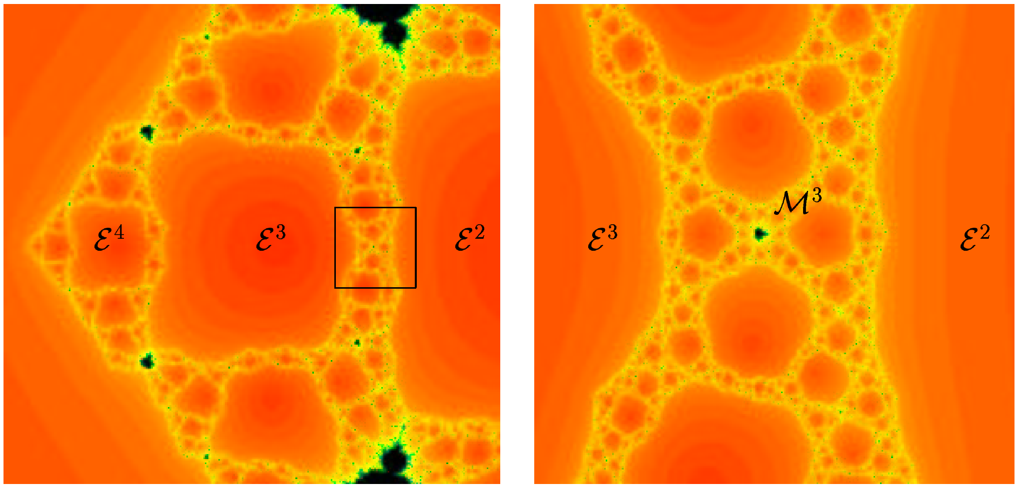

Figure 6: The Mandelpinski arc along the negative real axis. The $\mathcal{M}^k$ are so small that they are not visible in this picture. However, the magnification shows $\mathcal{M}^3$.

$j > k$ and $\mathcal{E}^j$ with $j \geq k$. And there is a finite Mandelpinski spoke lying on the other side of $\mathcal{M}^k$ which now contains finitely many sets $\mathcal{M}^j$ where $2 \leq j < k$ and $\mathcal{E}^j$ where $1 \leq j < k$. These will be the initial portions of two of the (eventually infinite) Mandelpinski spokes emanating from $\mathcal{M}^k$.

In this next phase of the construction, we shall show that, on each side of the Mandelbrot set $\mathcal{M}^k$ in the first spoke, there are a pair of infinite spokes, each extending over to one of the adjacent Sierpinski holes $\mathcal{E}^k$ and $\mathcal{E}^{k-1}$. We think of this as extending the two previously constructed spokes emanating from $\mathcal{M}^k$. In addition, we shall show that there are a pair of new finite spokes extending above and below each $\mathcal{M}^k$. These will be the initial portions of the first four spokes emanating from $\mathcal{M}^k$.

To begin this phase of the construction, let us assume that the critical value v_0^λ now lies in a particular open disk D_λ^k for some fixed $k \geq 2$. Let

$\mathcal{O}_k \subset \mathcal{O}'$ denote the set of parameters for which this happens. Now the boundary of D_λ^k is mapped by F_λ^{k-1} one-to-one onto the boundary of L^λ, and the boundary of L^λ varies analytically with λ. So we can construct a natural parametrization of this boundary which also varies analytically with λ. Then we can pull back this parameterization to the boundary of each D_λ^k. Again, as we saw earlier, as λ rotates around the boundary of the original disk $\mathcal{O}'$ in the parameter plane, v_0^λ rotates once around the boundary of R^λ. Hence, arguing just as in the previous section, there must be a unique parameter λ for which v_0^λ lands on any given point in the parametrization of the boundary of D_λ^k. Hence we have that $\mathcal{O}_k$ is a disk contained inside $\mathcal{O}'$ and, as λ rotates once around the boundary of $\mathcal{O}_k$, the critical value has winding number one around the boundary of the disk D_λ^k.

Now consider the set of preimages in L^λ of all of the D_λ^j and E_λ^j under F_λ. Since we have assumed that v_0^λ lies in D_λ^k, it follows that there is a unique preimage of D_λ^k in L^λ which is a disk that contains c_0^λ and is mapped two-to-one onto D_λ^k. Call this special disk L_k^λ. For each other D_λ^j (with $j \neq k$), there are now two preimage disks lying in L^λ. Note that, when $\lambda \in \mathbb{R}^-$ and $j > k$, there are a pair of preimages of D_λ^j lying along $\mathbb{R}^-$, one to the right of L_k^λ and one to the left. These preimages tend away from D_λ^k in either direction as j increases. When $2 \leq j < k$, there are again two preimages of D_λ^j, but when $\lambda \in \mathbb{R}^-$, these preimages no longer lie on the negative axis; rather they branch out more or less perpendicularly above and below L_k^λ on this axis. As for the preimages of E_λ^j in L^λ, we have the same situation: there are infinitely many pairs of preimages of each E_λ^j lying along $\mathbb{R}^-$ on either side of the preimage of D_λ^k when $j \geq k$ and $\lambda \in \mathbb{R}^-$, and finitely many pairs extending above and below this preimage when $1 \leq j < k$. Thus we have a pair of infinite chains of alternating preimages of the disks D_λ^k and E_λ^k extending away from L_k^λ in the wedge L^λ and another pair of chains consisting of finitely many such preimages extending in a "perpendicular" direction away from L_λ^k.

Since F_λ^{k-1} maps D_λ^k one-to-one over L^λ, we thus have a similar collection of preimages that lie inside the disk D_λ^k. We denote by D_λ^{kj} each of the two disks in D_λ^k that are mapped onto D_λ^j by F_λ^k when $j \neq k$. And we let D_λ^{kk} denote the single preimage of D_λ^k under F_λ^k that is contained in D_λ^k. Points in D_λ^{kj} have orbits that remain in R^λ for the first $k-2$ iterations, then map into L^λ under the next iteration, and then map into D_λ^j under the next iteration. Then F_λ^{j-1} maps this set of points onto L^λ. So F_λ^{k+j-1} maps each D_λ^{kj} one-to-one onto all of L^λ (assuming $k \neq j$). Then the next iteration takes this set two-to-one onto all of R^λ. Now the critical value for F_λ^{k+j} is again v_0^λ, and, as we showed above, as λ rotates around the boundary of $\mathcal{O}_k$, v_0^λ circles around the boundary of D_λ^k. Hence F_λ^{j+k} is polynomial-like of degree two on each of the two disks D_λ^{kj} (where we again emphasize that we are assuming $j \geq 2$ and $j \neq k$). So this produces a pair of Mandelbrot sets $\mathcal{M}^{kj}$ with base period $k+j$ in $\mathcal{O}_k$. As in the previous construction, the Mandelbrot sets $\mathcal{M}^{kj}$ with $j > k$ all have spines lying along $\mathbb{R}^-$, one on each side of $\mathcal{M}^k$. The other Mandelbrot sets with $j < k$ now lie off the real axis, one above $\mathcal{M}^k$ and the other below $\mathcal{M}^k$.

Similar arguments as in the preceding section also produce a pair of Sierpinski holes $\mathcal{E}^{kj}$ on each side of $\mathcal{M}^k$ along the real axis where now $j \geq k$. And there are a pair of Sierpinski holes $\mathcal{E}^{kj}$, one above and one below $\mathcal{M}^k$, where now $1 \leq j < k$. As earlier, these Mandelbrot sets and Sierpinski holes alternate along each of these spokes. See Figure 7. For parameters in the Sierpinski hole $\mathcal{E}^{k1}$, the critical orbit $F_\lambda^i(c_0^\lambda)$ lies in R^λ for iterations $1 \leq i \leq k-1$. Then $F_\lambda^k(c_0^\lambda)$ returns to L^λ, and then $F_\lambda^{k+1}(c_0^\lambda)$ enters T_λ.

We now sketch the construction of the other Mandelpinski spokes by induction. For simplicity, we will only consider the next phase of the construction; all subsequent phases follow in exactly the same way. This time

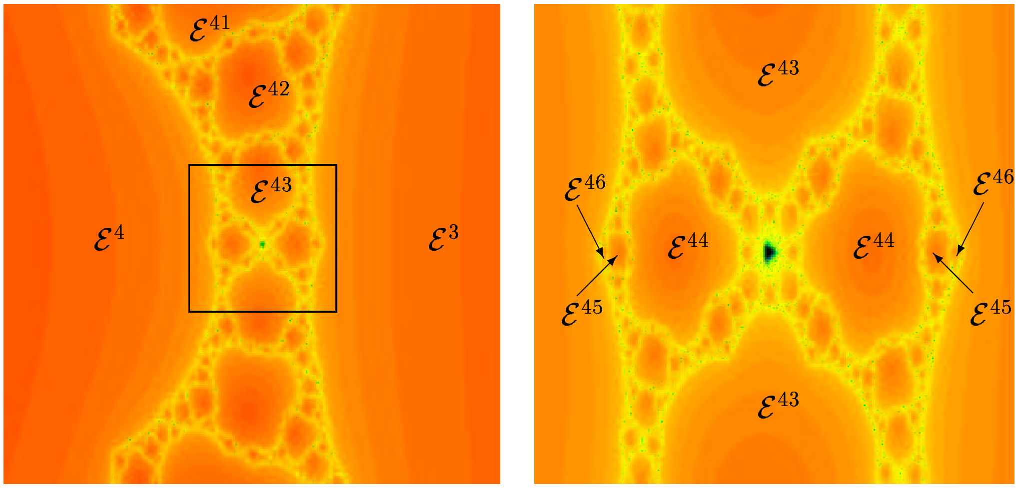

Figure 7: The finite spoke above and below $\mathcal{M}^4$ as well as a magnification showing the pair of infinite spokes along the real axis.

we will adjoin four infinite spokes that lie closer to $\mathcal{M}^k$ to those already in place, and then we will add four new finite spokes in betwen each of these infinite spokes.

To be precise, in the previous phase, we assumed that the critical value resided in a particular disk D_λ^k, and so there was a special disk $D_\lambda^{kk} \subset D_\lambda^k$ that was mapped two-to-one onto D_λ^k by F_λ^k. At this stage we make the further assumption that v_0^λ lies in D_λ^{kk}. Let $\mathcal{O}_{kk} \subset \mathcal{O}_k$ be the set of parameters for which this occurs. Note that $\mathcal{M}^k$ lies in $\mathcal{O}_{kk}$. We have that F_λ^k maps the boundary of D_λ^{kk} two-to-one onto the boundary of D_λ^k. Thus we may pull back the parametrization of ∂D_λ^k constructed earlier to produce a natural parametrization of ∂D_λ^{kk} which varies analytically with λ. Thus there is a unique λ for which v_0^λ lands on a given point in the boundary of D_λ^{kk}, and so, as λ winds once around the boundary of $\mathcal{O}_{kk}$, v_0^λ winds once around ∂D_λ^{kk}.

By the prior construction, we have a pair of infinite chains each of which consists of the disks D_λ^{kj} with $j > k$ and E_λ^{kj} with $j \geq k$ lying in the annular region $D_\lambda^k - D_\lambda^{kk}$ as well as a pair of finite chains consisting of the disks D_λ^{kj} and E_λ^{kj} with $j < k$ lying in the same annulus. Since F_λ^k maps D_λ^{kk} two-to-one onto the entire disk D_λ^k, we therefore have four new infinite chains inside D_λ^{kk} that are the preimages of the two infinite chains in the annular region. These chains consist of disks that we denote by either D_λ^{kkj} with $j > k$ or E_λ^{kkj} with $j \geq k$. Each of these chains then connects to one of the two infinite or finite chains already constructed in the outer annular region. This follows since these outer chains were all mapped onto the left or right portion of the original chain by F_λ^k. We also have four finite chains in D_λ^{kk} consisting of disks D_λ^{kkj} and E_λ^{kkj} with $j < k$ that are preimages of the finite chains in the annular region. These chains do not connect to the previously constructed chains in the annular region.

Then the same arguments as above produce the corresponding spokes in the parameter plane. Each of the two finite and infinite spokes constructed earlier now have an added infinite spoke that lies in the region between $\mathcal{M}^k$ and that spoke. The Mandelbrot sets and Sierpinski holes in this new portion of the spoke are given by $\mathcal{M}^{kkj}$ where $j > k$ and $\mathcal{E}^{kkj}$ where $j \geq k$ and the four new finite spokes consist of similar sets with now $j < k$. These are all associated with rays of angle $\ell/8$ with ℓ even for the infinite spokes and ℓ odd for the finite spokes.

At this stage we now have eight Mandelpinski spokes emanating from $\mathcal{M}^k$, four finite spokes and four infinite spokes. Continuing inductively, at the next stage, we then add eight infinite spokes between each of these spokes and $\mathcal{M}^k$ as well as eight new finite spokes, one between each of these newly added infinite spokes. In the limit, we get an infinite collection of Mandelpinski spokes emanating from $\mathcal{M}^k$.

5 The Mandelpinski Maze

In this section we further elaborate on the construction of the Mandelbrot sets and Sierpinski holes in the parameter plane of F_λ by constructing what we call a *Mandelpinski maze.* In the previous sections, we actually constructed the first two portions of this maze. We first showed the existence of a string of interspersed Mandelbrot sets $\mathcal{M}^k$ with $k \geq 2$ and Sierpinski holes $\mathcal{E}^1$ with $k \geq 1$ along the real axis in the parameter plane. Next, we showed that, between each $\mathcal{E}^{k-1}$ and $\mathcal{E}^k$, there exist a pair of infinite spokes, each containing Mandelbrot sets $\mathcal{M}^{kj}$ where $j > k$ and Sierpinski holes $\mathcal{E}^{kj}$ where $j \geq k$ in the same alternating arrangement as earlier. One spoke extends from $\mathcal{M}^k$ to $\mathcal{E}^{k-1}$, the other from $\mathcal{M}^k$ to $\mathcal{E}^k$. The are also a pair of finite spokes extending away from $\mathcal{M}^k$ in opposite directions. These finite spokes contain the Mandelbrot sets $\mathcal{M}^{kj}$ where $2 \leq j < k$ and the Sierpinski holes $\mathcal{E}^{kj}$ where now $1 \leq j < k$. We think of this second collection of spokes emanating from $\mathcal{M}^k$ as a "plus sign" centered at $\mathcal{M}^k$.

In the previous construction we assumed that the critical value lies in the disk D^{kk}. Now we change this assumption so that the critical value now lies in either of the two disks D^{kj} where now $j \neq k$.

Recall that it is when $\lambda \in \mathcal{O}_k$ that the critical value v_0^λ lies in D_λ^k and that L_λ^k is the preimage of D_λ^k in L^λ that contains c_0^λ. In the previous construction, for each $j > 1$ and $j \neq k$, we produced a pair of disks $D_\lambda^{kj} \subset D_\lambda^k$, and then we showed that F_λ^{k+j} was a polynomial-like map of degree two on D_λ^{kj}. This generated a pair of Mandelbrot sets that we called $\mathcal{M}^{kj}$. So fix k and j and concentrate on one of the two disks D_λ^{kj} and hence, in the parameter plane, on the corresponding Mandelbrot set $\mathcal{M}^{kj}$. As in the previous step, we now assume that v_0^λ lies in this disk D_λ^{kj}. This is possible since we have shown that v_0^λ winds once around the boundary of D_λ^k as λ winds around

$\partial\mathcal{O}_k$, and $D_\lambda^{kj} \subset D_\lambda^k$. Let $\mathcal{O}_{kj}$ be the set of parameters for which this occurs. Then F_λ^{j+k-1} maps D_λ^{kj} one-to-one over L^λ. Thus we can pull back the earlier parametrization of the boundary of L^λ to construct an analytic parameterization of the boundary of D_λ^{kj}. Just as before, there then exists a unique λ in the boundary of $\mathcal{O}_{kj}$ for which v_0^λ lands on a given point on this parametrized boundary curve. Hence v_0^λ winds once around the boundary of the disk D_λ^{kj} as λ winds once around the boundary of $\mathcal{O}_{kj}$.

Since v_0^λ lies in D_λ^{kj}, there is then a preimage of the structure of all of the disks $D_\lambda^{k\ell}$ and $E_\lambda^{k\ell}$ contained in D_λ^k that now lies in the preimage of D_λ^k in L^λ, namely, L_λ^k. Each $D_\lambda^{k\ell}$ and $E_\lambda^{k\ell}$ now has two preimages in L_λ^k, with the exception of the chosen D_λ^{kj}, which has only one preimage that contains the critical point c_0^λ. Thus we again "duplicate" the preimage structure that we see in D_λ^k in the region L_λ^k, and center this duplication around the preimage of D_λ^{kj}. Then F_λ^{k+j-1} maps the disk D_λ^{kj} one-to-one onto L^λ since $j \neq k$. Hence there is a copy of this duplicated preimage structure that we see in L^λ that is now contained in the chosen disk D_λ^{kj}. Thus, for each $\ell > 1$, we now have four disks named $D^{kj\ell}$ that are contained in D_λ^{kj}. Each of the $D_\lambda^{kj\ell}$ is mapped one-to-one onto L^λ by $F_\lambda^{k+j+\ell-1}$ and hence two-to-one over themselves by $F_\lambda^{k+j+\ell}$. Then, arguing as before, this map is polynomial-like of degree two on each $D^{kj\ell}$ and this produces four new baby Mandelbrot sets $\mathcal{M}^{kj\ell}$ which are arranged in a similar pattern as the preimages of the disks in the dynamical plane. Similar arguments also yield four Sierpinski holes $\mathcal{E}^{kj\ell}$.

Note also that the maze structure in the small neighborhood of $\mathcal{M}^{kj}$ is now more complicated than before. For example, if we had chosen the disk D_λ^{kj} to be one of the disks in one of the two finite chains of disks emanating from D_λ^k, then the maze structure around $\mathcal{M}^{kj}$ would consist of a pair of finite spokes, one on each side of $\mathcal{M}^{kj}$, and also a pair of "plus signs," each again on opposite sides of $\mathcal{M}^{kj}$. On the other hand, had D_λ^{kj} been chosen to be one of the disks in the infinite string of disks, then there would now be a pair of infinite spokes emanating from $\mathcal{M}^{kj}$ and again a pair of "plus signs."

Then we may continue this process, each time selecting a previously constructed Mandelbrot set with itinerary $s_0 \ldots s_n$. Assuming the sequence $s_0 \ldots s_n$ is not a repeated finite sequence, i.e., not a repeating sequence of the form $s_0 \ldots s_j \ldots s_0 \ldots s_j$, this inductive process then produces the more intricate maze structure around the given Mandelbrot set.

6 Open Questions

One open problem in this area is to determine the exact structure of the Mandelpinski maze. One should think of this at the m^{th} stage as a graph with the vertices representing the Mandelbrot sets (and between each pair of connected vertices there is a unique Sierpinski hole). How this graph looks changes at each vertex at each stage. The question is how to sketch the graph at each stage and, then, how to describe the limiting "graph." Another open problem is to determine the exact structure of the entire spoke along, say, the negative real axis. We produced infinitely many Mandelbrot sets and Sierpinski holes along this axis, but what remains in the limit? Clearly, these are parameters for which the critical orbit has an infinite itinerary that is neither periodic nor escaping. Are all such parameters just singletons? We conjecture that the answer is yes.

References

[1] Cuzzocreo, D. and Devaney, R. L. Simple Mandelpinski Necklaces for $z^2 + C/z^2$. To appear.

[2] Devaney, R. L. Baby Mandelbrot Sets Adorned with Halos in Families of Rational Maps. In *Complex Dynamics; Twenty-Five Years After the Appearance of the Mandelbrot Set*. Amer. Math. Soc. Contemporary Math. **396** (2006), 37-50.

[3] Devaney, R. L. Structure of the McMullen Domain in the Parameter Space of Rational Maps. *Funda. Math.* **185** (2005), 267-285.

[4] Devaney, R. L. Singular Perturbations of Complex Polynomials. *Bulletin of the AMS* **50** (2013), 391-429.

[5] Devaney, R. L. A Mandelpinski Maze for Rational Maps of the Form $z^n + \lambda/z^d$. To appear in *Indagationes Math.*

[6] Devaney, R. L. Mandelpinski Spokes in a Family of Rational Maps. To appear in *JDEA*.

[7] Devaney, R. L. Cantor Necklaces and Sierpinski Curve Julia Sets. *Qual. Thy. Dyn. Sys.* **5** (2004), 337-359.

[8] Devaney, R. L. The McMullen Domain: Satellite Mandelbrot Sets and Sierpinski Holes. *Conformal Geometry and Dynamics* **11** (2007), 164-190.

[9] Devaney, R. L., Jang, H. J., So, Y. N., and Marotta, S. Generalized Baby Mandelbrot Sets Adorned with Halos in Families of Rational Maps. To appear.

[10] Devaney, R. L. and Look, D. M. A Criterion for Sierpinski Curve Julia Sets. *Topology Proceedings* **30** (2006), 163-179.

[11] Devaney, R. L. and Look, D. M. Buried Sierpinski Curve Julia Sets. *Discrete and Continuous Dynamical Systems* **11** (2005), 1035-1046.

[12] Devaney, R. L., Look, D. M., and Uminsky, D. The Escape Trichotomy for Singularly Perturbed Rational Maps. *Ind. Univ. Math. J.* **54** (2005), 1621-1634.

[13] Devaney, R. L. and Marotta, S. The McMullen Domain: Rings Around the Boundary. *Trans. Amer. Math. Soc.* **359** (2007), 3251-3273.

[14] Devaney, R. L. and Pilgrim, K. Dynamic Classification of Escape Time Sierpinski Curve Julia Sets. *Funda. Math.* **202** (2009), 181-198.

[15] Devaney, R. L. and Russell, E. Connectivity of Julia Sets of Singularly Perturbed Rational Maps. In *Chaos, CNN, Memristors and Beyond.* World Scientific Press (2013), 239-245.

[16] Douady, A. and Hubbard, J. On the Dynamics of Polynomial-like Mappings. *Ann. Sci. ENS Paris* **18** (1985), 287-343.

[17] McMullen, C. Automorphisms of Rational Maps. *Holomorphic Functions and Moduli.* Vol. 1. Math. Sci. Res. Inst. Publ. **10** Springer, New York, 1988.

[18] Milnor, J. *Dynamics in One Complex Variable.* Princeton University Press, 2006.

[19] Moreno Rocha, M. A Combinatorial Invariant for Escape Time Sierpinski Rational Maps. *Funda. Math.* **222** (2013), 99-130.

[20] Roesch, P. On Capture Zones for the Family $f_\lambda(z) = z^2 + \lambda/z^2$. In *Dynamics on the Riemann Sphere*. European Mathematical Society (2006), 121-130.

[21] Whyburn, G. T. Topological Characterization of the Sierpinski Curve. *Funda. Math.* **45** (1958), 320-324.